Chapter 2
Overview of Energy Harvesting Technologies

Harvesting or scavenging mechanical energy from the surroundings is a potential strategy to develop self-powered sensor nodes and electronic devices. In this chapter, a literature review is presented for various mechanical energy harvesting technologies to understand the state-of-the-art. The first part of the chapter discusses commonly used principles to convert mechanical energy into electrical energy. Basic physics and working all the mechanisms have been explained and previously developed devices by other research groups have been reviewed.

The second part of the chapter reviews the progress in the area of TENGs. Different working mechanisms, materials and fabrication techniques utilized for TENG devices have been reviewed. Thereafter, applications of TENG devices to harvest mechanical energy in different forms e.g. biomechanical energy, vibration energy and wind energy, has been discussed. Triboelectric mechanism also has immense applications in the area of sensing. Triboelectric mechanism has been reviewed for various type of self-powered sensors e.g. pressure sensors, vibration sensors, motion tracking systems, chemical sensors etc.

2.1 Mechanical Energy Harvesting Mechanisms

2.1.1 Piezoelectric Energy Harvesters

Piezoelectric mechanism is the most common and well researched technique in the area of mechanical energy harvesters. These devices work on the property of material known as piezoelectricity. It is the property of the materials to produce charge (or voltage) when stimulated by a mechanical stress. Some of the popular materials which exhibit piezoelectricity are quartz, lead zirconate titanate (PZT), aluminum nitride (AlN), zinc oxide (ZnO) and polyvinylidene fluoride (PVDF). Piezoelectric effect can be explained using a molecular model as shown in Fig. 2.1.

L. Dhakar, *Triboelectric Devices for Power Generation and Self-Powered Sensing Applications*, Springer Theses,
DOI 10.1007/978-981-10-3815-0_2

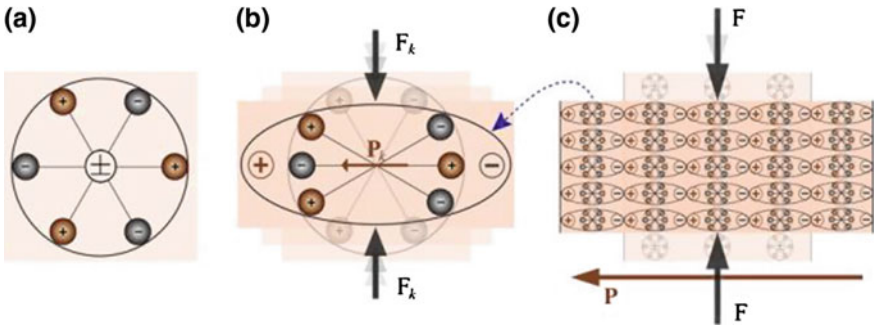

Fig. 2.1 Piezoelectricity explained using a molecular model. **a** A molecule in an undisturbed state without any external force. **b** The molecule becomes polarized due to an external force F_k applied. **c** Molecules in a piezoelectric material collectively leading to generation of voltage due to polarization when an external force is applied [1]

In Fig. 2.1a, the molecule is in undisturbed state, but as an external force F_k is applied, it causes unbalance of charge leading to creation of a small dipole P_k as shown in Fig. 2.1b. Collectively, all these small dipoles create a dipole P in the material. This phenomenon in materials is known as piezoelectricity.

Researchers have utilized the piezoelectric effect to harvest mechanical energy and convert it into electrical energy. The most common configuration and design used for piezoelectric energy harvester (PEH) is using a cantilever [2, 3]. A typical configuration of cantilever based PEH is shown in Fig. 2.2. The piezoelectric cantilever undergoes cycle of compression and tension as it is excited through external vibration or cyclic force. This cyclic force results into generation of cyclic voltage signal across the cantilever electrodes across the piezoelectric layer. A proof mass (M) at the tip of the cantilever beam is typically used to improve the stress levels in the piezoelectric layer. This results in a higher magnitude of the voltage generated at the electrodes.

Renaud et al. [4] used a microelectromechanical system (MEMS) based PZT cantilever design to harvest vibrational energy. The major limitation of cantilever

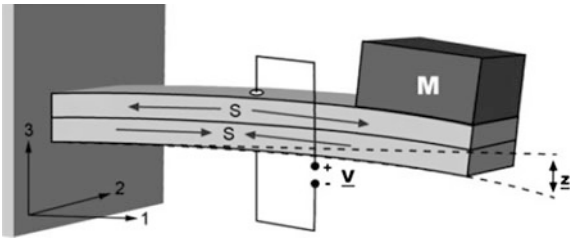

Fig. 2.2 Schematic of a typical cantilever based PEH. S is the strain in the piezoelectric layer shown with directional arrows, V is the generated voltage, M is the proof mass and z is vertical displacement of the cantilever tip [2]

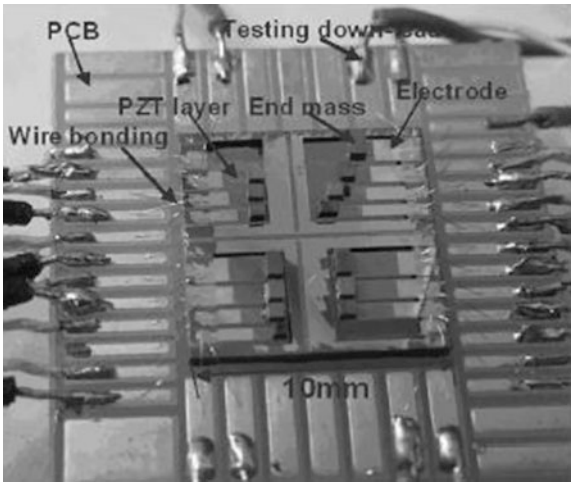

Fig. 2.3 Array of cantilevers used to improve the operating bandwidth of the vibrational PEH [5]

based PEH is the limited frequency range in which these devices can operate due to resonant behavior. Liu et al. [5] used an array of PZT cantilevers (Fig. 2.3) with different mechanical dimensions and hence different resonant frequencies to improve the operating bandwidth of the devices.

Apart from the cantilever based designs of PEH devices, researchers have used piezoelectric materials for demonstrations in many practical applications. Kymissis et al. [6] from MIT Media Laboratory first demonstrated shoe based energy harvesting system in 1998 using PZT and PVDF for wearable applications. The image of the prototype device is shown in Fig. 2.4. The prototype was demonstrated to generate enough power to for a radio-frequency identification (RFID) tag. A windmill based piezoelectric energy harvesting was developed by Priya [7] using 10 piezoelectric bimorphs which were actuated using a windmill.

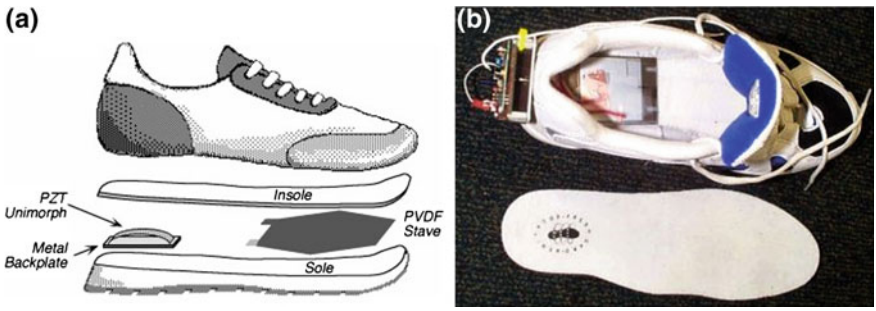

Fig. 2.4 **a** Schematic diagram of the shoe based energy harvesting device. **b** Photograph of the fabricated prototype [6]

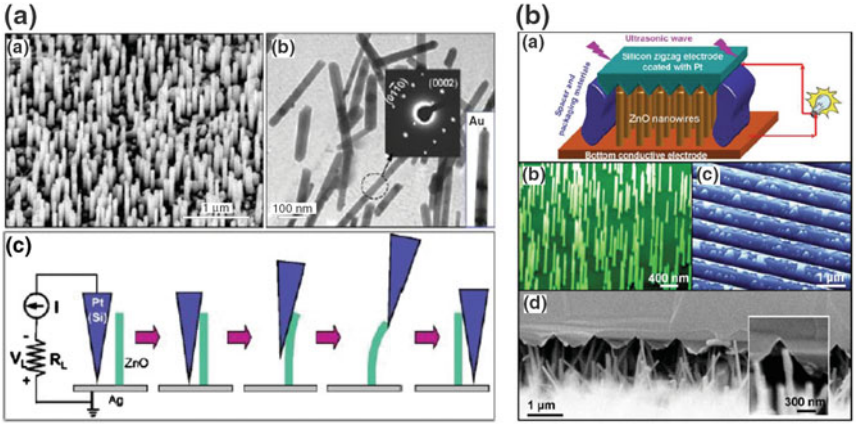

Fig. 2.5 **a** ZnO nanowires actuated using Pt coated AFM tip [8]. **b** Pt coated AFM tip replaced by a zigzag Pt electrode actuated using ultrasonic waves [9]

ZnO nanowire based energy harvester was first demonstrated by Wang and Song [8] using array of aligned nanowires (Fig. 2.5a). The nanowires were deflected with a conductive atomic force microscope (AFM) tip in contact mode. To improve the practical application of the concept, the Pt coated AFM tips were replaced by microfabricated zigzag shaped Pt electrodes as shown in Fig. 2.5b [9]. Chung et al. [10] fabricated ZnO thin film on a polyethylene terephthalate (PET) substrate using simple reactive zinc hydroxo-condensation process (Fig. 2.6a). This device was demonstrated to be suited for human wearable energy harvesting devices. Lee et al. [11] fabricated a flexible and conformable ZnO nanowire based piezoelectric nanogenerator in an aluminum (Al) foil coated with Polymethyl methacrylate (PMMA) (Fig. 2.6a). The device could generate an output voltage and current of up to 50 mV and 200 nA respectively, by utilizing fluttering motion generated through wind energy. Lin et al. [12] demonstrated a transparent flexible nanogenerator by growing ZnO nanowires on a PDMS substrate. The generated an output voltage and

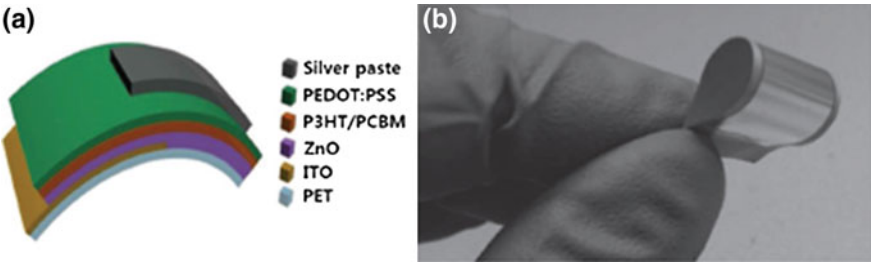

Fig. 2.6 **a** Schematic diagram of the ZnO film based piezoelectric nanogenerator on PET substrate [10]. **b** Photograph of the super flexible piezoelectric nanogenerator [11]

current of 8 V and 0.5 μA, respectively, with a power output density of 5.3 mW/cm^3. The device was also demonstrated as a self-powered sensor to monitor vehicle speed and detect vehicle weight.

Research breakthroughs in the area of novel fabrication techniques for piezoelectric materials have found applications in the area of wearable and flexible energy harvesting devices. But limited choice of materials and complex fabrication techniques still remain one of important challenges for piezoelectric energy harvesting devices. These fabrication challenges have been a bottleneck to find application implantable, biocompatible and wearable energy harvesters, which can be commercialized.

2.1.2 Electromagnetic Energy Harvesters

Electromagnetic mechanical energy harvesters work on the principle of Faraday's law of induction. Majority of the electrical motors, transformers, inductors and generators are based on this fundamental operating principle. Faraday's law states that the voltage or electromotive force (emf) generated in a closed circuit directly proportional to the total flux through the closed loop circuit. The equation for Faraday's law is given by:

$$V = -\frac{d\Phi}{dt} \tag{2.1}$$

where V the voltage is induced across the two ends of closed circuit, Φ is total flux and t is time. If there are total N coils in the circuit, total flux Φ is given by:

$$\Phi = \sum_{i=1}^{N} \int_{A_i} B.dA \tag{2.2}$$

where B is the magnetic field and A_i is the area of the ith coil. Faraday's law has been extensively used in large sized commercial generators to produce power using fuel, hydropower and other traditional sources. Same principle can be utilized to harvest mechanical energy at a much smaller scale. Williams et al. [13] demonstrated one of the first micro scale electromagnetic energy harvester using a samarium-cobalt permanent magnet and planar gold (Au) coils. Lee et al. [14] demonstrated a AA battery sized electromagnetic energy harvester using laser micromachining as a fabrication technique (Fig. 2.7a). Same research group also demonstrated an electromagnetic energy harvester capable of harvesting energy from different resonant modes as shown in Fig. 2.7b.

Kulkarni et al. [18] developed a micro energy harvester by using electrodeposited copper coils and NdFeB magnetics. The device had a small volume of 0.1 cm^3 and could generated a power of 586 nW across a load resistance of 110 Ω at an acceleration of 8.829 m/s^2. Cepnik and Wallrabe [16] designed a flat

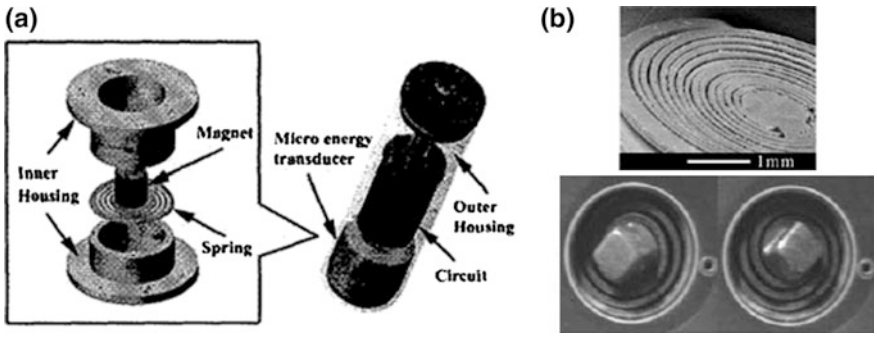

Fig. 2.7 **a** AA size micro energy harvester by Lee et al. [14]. **b** Multi-modal energy harvester developed by Chin et al. [15]

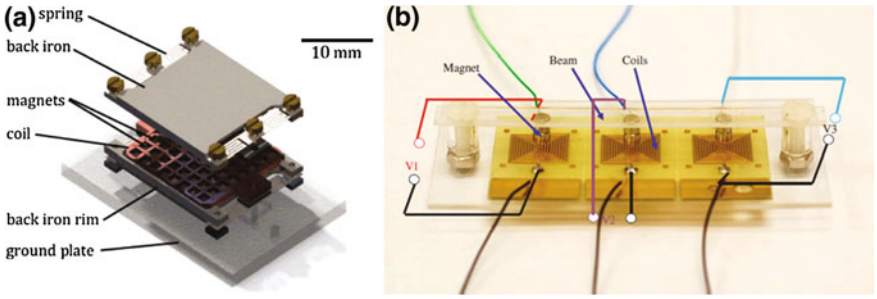

Fig. 2.8 **a** A flat energy harvester using serpentine springs for in-plane movement [16]. **b** A low cost electromagnetic energy harvester using coils etched on a printed circuit board (PCB) [17]

electromagnetic energy harvester which used micro fabricated serpentine springs for in-plane movement. The device as shown in Fig. 2.8a generated an average power of 12 μW at an acceleration of 1 ms^{-2}. Yang et al. [17] used an acrylic fixed-fixed beam with three permanent magnets attached to it. Correspondingly, three coils were fabricated on a printed a printed circuit board (PCB) and placed beneath the permanent magnets as shown in Fig. 2.8b. As the beam was excited using vibrations, it generated power from different vibration modes of the beam. The maximum power produced by device was demonstrated to be 3.2 μW.

Donelan et al. [19] demonstrated a complete working prototype of a biomechanical energy harvester using electromagnetic energy harvesting technique. The device was designed for applications for powered prosthetic limbs and charging medical devices (Fig. 2.9). The electromagnetic mechanism based energy harvesters have advantage of very low device impedance as compared to piezoelectric, electrostatic and triboelectric energy harvesting devices. These devices are suitable for large scale energy production but as the size of the device decreases, the coil and magnet fabrication becomes a huge challenge.

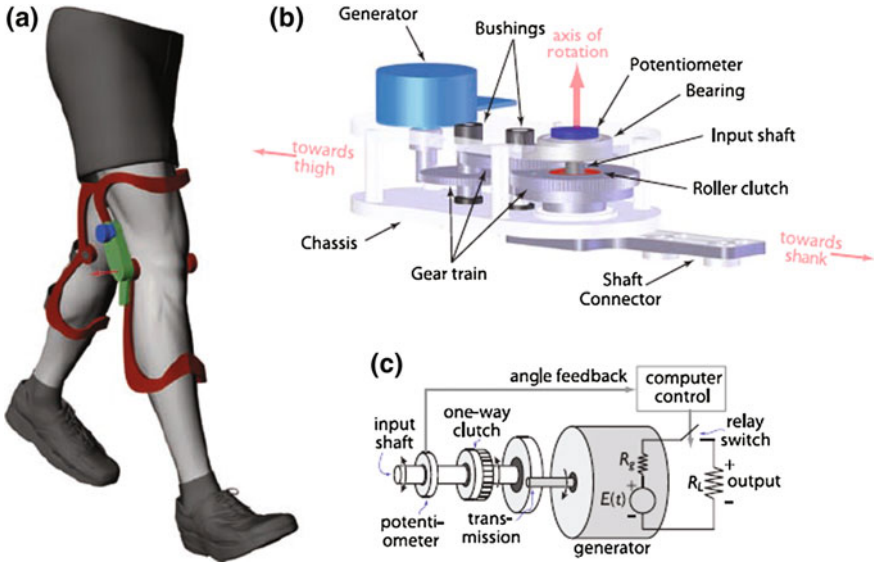

Fig. 2.9 Biomechanical energy harvester to harvest energy during human walking for applications in prosthetic limbs [19]

2.1.3 Electrostatic Energy Harvesters

Electrostatic energy harvesters work on the principle of variable parallel plate capacitor. The mechanical energy available in the surroundings is used to change the gap between two parallel plates, which together form the capacitor system. This change in the gap or relative position of the two plates leads to flow of charges in the external load connected across the two plates. The physical mechanism of the electrostatic energy harvesters can be distinguished based on the type of relative motion between the two plates as shown in Fig. 2.10.

Electrostatic energy harvesters can be divided into categories: (i) using external voltage supply for biasing (ii) using electrets. The first category of the devices rely on an external bias to create a potential difference between the two parallel plates. In the second type of device, electrets are used to create a potential difference between the parallel plates. Electrets are essentially dielectric materials with permanent electrical polarization analogous to permanent magnet.

Meninger et al. [21] proposed one of the first energy harvesters based on the electrostatic mechanism. To improve the overall capacitance per unit displacement of the moving part, Hoffmann et al. [22] used triangular electrode design as shown in Fig. 2.11a. Yang et al. [23] demonstrated a rotary comb based energy harvester design for planar vibrations. The device produced a maximum power of 2.5 μW at an acceleration of 2.5 g. Nguyen et al. [24], Nguyen and Halvorsen [25] proposed and demonstrated the concept of utilizing non-linear springs as shown in Fig. 2.12b

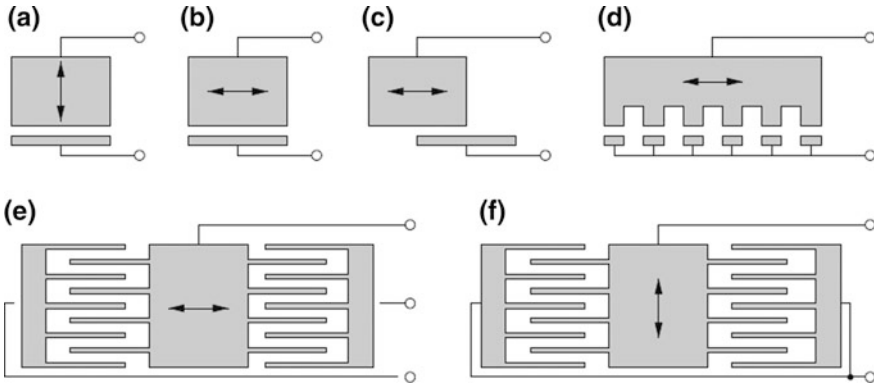

Fig. 2.10 **a–f** Various configurations used for electrostatic energy harvesters. The *arrows* depict the direction of relative motion between the fixed and moving part [20]

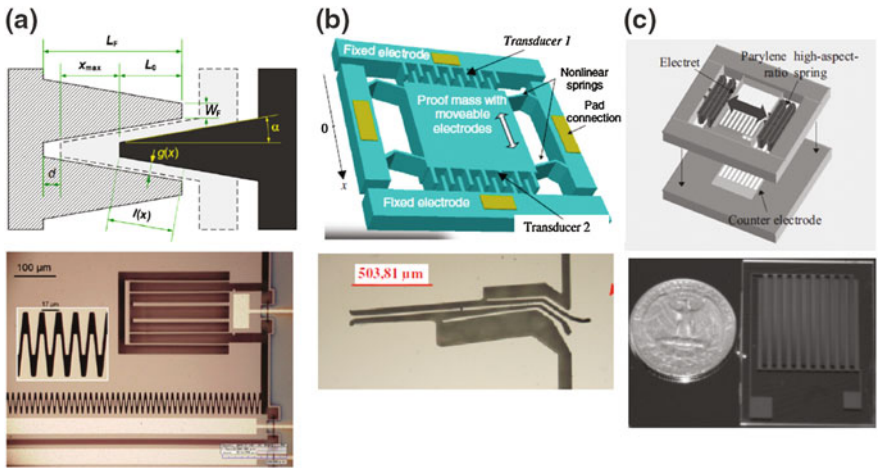

Fig. 2.11 **a** Triangular electrodes used in the electrostatic energy harvesters to increase the capacitance change per unit of displacement [22]. **b** Non-linear springs to improve the operating bandwidth of vibration based electrostatic energy harvesters [24]. **c** Vibrational energy harvester using CYTOP electret [27]

to improve the operating frequency bandwidth of the device. The non-linear springs were designed to exhibit softening in leading to wideband characteristics and higher output power.

Boland et al. [26] proposed a micro fabricated Teflon electret based energy harvester utilizing rotation mechanism. The rotational electrostatic energy harvester generated a power of 25 µW. Tsutsumino et al. [27] used a CYTOP based electret to harvest vibrational energy which could produce a power of up to 38 µW (Fig. 2.11c). They later improved the surface charge density of the electrodes by the

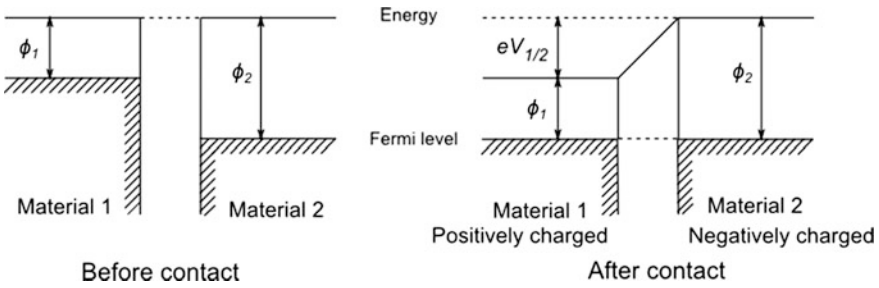

Fig. 2.12 Charge transfer due to the difference in work function between two metal for metal-metal contact [29]

addition of amidosilyl end group [28]. The improved device generated power output up to 0.7 mW.

The electrostatic energy harvesters are not the most popular solution for mechanical energy harvesting because of their low power output as compared to other mechanisms. Moreover, electret less electrostatic energy harvesters need an external voltage supply which is not suitable for self-powered wireless nodes. On the other hand, electret based electrostatic energy harvesters retain the charges only for a limited period of time.

2.2 Triboelectric Energy Harvesting

Triboelectric energy harvesters utilize two principles working in conjunction: triboelectric effect and electrostatic induction. Triboelectric effect is a type of contact electrification which leads to charging of two surfaces when there are put in contact with each other. Many theories have been proposed in literature to explain the phenomenon of contact electrification [29]. One of the well-established and accepted model to explain the concept of electron transfer is based on difference in work functions of various materials [30]. As per this model, as two metals come in contact with each other, the electrons transfer by tunneling in order to prevail the thermodynamic equilibrium. The potential difference $V_{1/2}$ generated between the two metals due to this charge transfer can be given by the following equation:

$$V_{1/2} = -\frac{(\phi_1 - \phi_2)}{e} \tag{2.3}$$

where $V_{1/2}$ is the contact potential difference of metal 1 against metal 2, ϕ_1 is the work function of metal 1, ϕ_2 is the work function of metal 2 and e is the elementary charge. The same theoretical model can be used to explain and understand the charge transfer in metal-insulator and insulator-insulator contact by using the

Fig. 2.13 Triboelectric series for various materials arranged in order of their tendency to attract or donate electrons

concept of effective work function for insulators [31, 32]. Figure 2.12 pictorially depicts this model given by Harper [30].

The charges generated during the contact electrification process are generated on the surface of the both the materials or triboelectric layers. Based on chemical structure and properties, various metals and dielectric materials have different tendencies to donate and accept electrons. Different metals and dielectric materials can be arranged in an order as per their tendency to donate or accept electrons. This order is known as triboelectric series [33, 34] and is shown in Fig. 2.13 for a limited number of materials. The materials on the positive side of the series have a tendency to donate electrons relative to the materials on negative side. This means that the materials on the positive side have propensity to get positive charged and vice versa. Relative positions of materials in triboelectric series can be used to predict and choose the polarity of charges generated when two material are put in contact with each other. Also farther the two triboelectric materials in series, higher is the surface charge density produced during the contact electrification process. This rule is important for selection of materials during the design of TENGs.

On the basis of mechanical operating principle, triboelectric mechanism for energy harvesting can broadly be divided into two categories: (i) Out-of-plane contact-separation mechanism (ii) in-plane sliding mechanism. The theory and working principle for both the mechanisms are explained in following sections.

2.2.1 Out-of-Plane Contact-Separation Mechanism

In out-of-plane mechanism the triboelectric layers undergo relative motion in the direction normal to the plane of contact. This relative motion results in contact and separation of the triboelectric layers. As the triboelectric layers come into contact with each other, both layers get charged with equal and opposite surface charge density σ due to contact electrification. The surface charges lead to induced charges on the metal electrodes in the energy harvesting device as shown in Fig. 2.14 [35]. As the two layers undergo relative motion i.e. separating or approaching due to

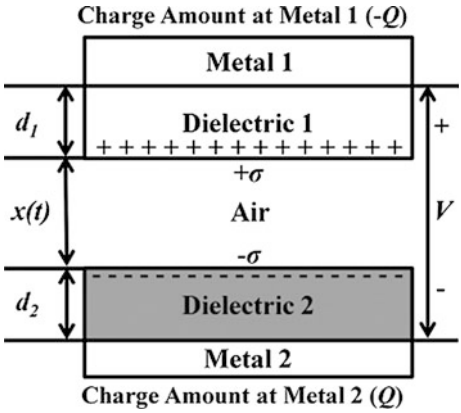

Fig. 2.14 Schematic of an out-of-plane contact-separation based triboelectric energy harvester [35]

external mechanical pressure/force, the relative potential between the two electrode changes. This change in relative potential leads to a current in the external load connected between the two electrodes. This system can be treated as a system of parallel plate capacitors and can be used to develop a theoretical model. In this case, working principle is essentially similar to the electrostatic energy harvester but the charges are internally generated using contact electrification instead of an externally power supply or using electrets. A general theoretical model for this mechanism was developed by Niu et al. [35]. As per the model, the open circuit voltage and short circuit current can be given by Eqs. (2.4) and (2.5), respectively.

$$V_{oc} = \frac{\sigma x(t)}{\varepsilon_0} \tag{2.4}$$

$$I_{SC} = \frac{S\sigma d_0 v(t)}{(d_0 + x(t))^2} \tag{2.5}$$

where V_{oc} is the open circuit voltage, σ is the surface charge density, $x(t)$ is the relative distance between two triboelectric layers, ε_0 is the dielectric constant of air, I_{SC} is the short circuit current, S is the area of triboelectric layer, $v(t)$ is the relative velocity of triboelectric layers, d_0 is defined as the effective thickness constant given by $\frac{d_1}{\varepsilon r_1} + \frac{d_2}{\varepsilon r_2}$. Here d_1 and d_2 are thickness of triboelectric layers 1 and 2, ε_{r1} and ε_{r2} are relative dielectric constants of triboelectric layers 1 and 2.

2.2.2 *In-Plane Sliding Mechanism*

As the name suggests, in-plane sliding mechanisms comprises of relative sliding motion between triboelectric layers. A schematic for in-plane sliding mechanism is shown in Fig. 2.15. As the two triboelectric layers are in contact there is an equal

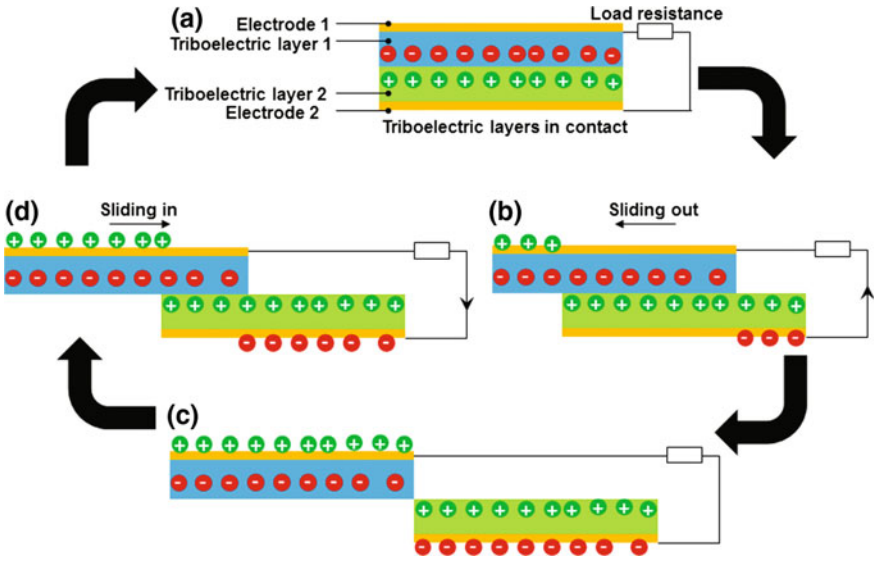

Fig. 2.15 Schematic for in-plane sliding mechanism based triboelectric energy harvester

and opposite surface charge generated on surface of both the layers. As triboelectric layer 1 moves out relative to triboelectric layer 2, there is a decrease in the contact area between two layers. This leads to charges induced in electrodes corresponding to balance the surface charges on both triboelectric layers. As both the electrodes are connected through a load resistor, there is a flow of electrons from top electrode to bottom electrode to balance the charges. This flow of electrons in the load resistor or current flow continues till the two triboelectric layers are completely separated as shown in Fig. 2.15c.

As the energy generation cycle continues, triboelectric layer 1 moves in relative to triboelectric layer 2 due to the external mechanical force. This leads to a flow of current in the external circuit in the opposite direction of sliding out process as shown in Fig. 2.15d. A theoretical model was proposed by Niu et al. [36] for the in-plane sliding mechanism based triboelectric energy harvester. According to the model, the open circuit voltage and short circuit current can be expressed by Eqs. (2.6) and (2.7).

$$V_{oc} = \frac{\sigma x}{\varepsilon_0 (l - x)} \left(\frac{d_1}{\varepsilon r_1} + \frac{d_2}{\varepsilon r_2} \right) \tag{2.6}$$

$$I_{SC} = \sigma w v(t) \tag{2.7}$$

where V_{oc} is the open circuit voltage, σ is the surface charge density, x is the relative separation distance between triboelectric layers in lateral direction, l is the length of

triboelectric layers in the direction of motion, ε_0 is the dielectric constant of air, d_1 and d_2 are thickness of triboelectric layers 1 and 2, ε_{r1} and ε_{r2} are the relative dielectric constants of triboelectric layers 1 and 2, I_{sc} is the short circuit current, $v(t)$ is the relative velocity of triboelectric layers, w is the width in the lateral direction perpendicular to motion direction of the triboelectric layer.

2.3 Materials and Fabrication of Triboelectric Nanogenerators

During the design of TENG devices, contact electrification process due to triboelectric effect can be engineered to improve the power generation performance. The performance of contact electrification majorly depends on two factors: (a) choice of triboelectric materials and (b) surface topography of the triboelectric layers. Choice of materials for triboelectric layers is important as it fundamentally affects the amount of surface charge generated due to triboelectric effect. The generated surface charge depends on the relative tendency of two triboelectric materials. Other practical factors affecting the choice of materials are cost, type of application, biocompatibility and fabrication limitations. In addition, surface topography is another crucial factor as it is predominantly responsible for defining effective contact area and charge separation during contact electrification due to triboelectric effect.

Researchers have used various materials as triboelectric layers based on the fabrication compatibility, cost and patternability. Another design step to improve the performance of TENGs is to deploy different fabrication techniques to achieve various type of micro/nano surface topographies to enhance the surface charge density during contact electrification. A summary is presented in Table 2.1 about these materials and topographies used to improve the device performance.

2.4 Triboelectric Energy Harvesters and Self-powered Sensors

One of the early prototype of TENG was reported in 2012 by Fan et al. [53] based on triboelectric mechanism as shown in Fig. 2.16a. A transparent and flexible energy harvester was demonstrated which used patterned PDMS films as triboelectric layer. Three patterns including line, cube and pyramid shaped structures were used to pattern PDMS films. It was demonstrated that plain film, line, cube and pyramid patterns based device had performance in the increasing order as depicted in Fig. 2.16b. The device generated a maximum output voltage and current of 18 V and 0.7 μA, respectively. The device was also demonstrated as a

Table 2.1 Materials and surface topographies for triboelectric energy harvesters

Material	Surface topography/processing	Reference
TiO_2	Nanowires and nanosheet	Lin et al. [37]
Al	Nanopores	Yang et al. [38]
PTFE	Nanowires	Yang et al. [38]
SiO_2	Nanoparticles	Cheng et al. [39]
PDMS	Pyramid shaped structures using molding	Han et al. [40]
Al	Nanostructures of average size ~200 nm	Han et al. [40]
PDMS	Nanowire	Yang et al. [41]
Si	Pyramid shaped texture	Yang et al. [41]
PTFE	Etched nanoparticle topography	Yang et al. [42]
Ag	Nanowire/nanoparticle composite	Lin et al. [43]
Fluorinated ethylene-propylene	Dry etched nanowire structures	Yang et al. [44]
Kapton	Dispersed with PTFE nanoparticles	Jing et al. [45]
PDMS	Micropillars	Yang et al. [46]
Al	Nanopores	Bai et al. [47]
Poly-vinylchloride	Nanowires	Du et al. [48]
Cu	Micro roughness by coating Cu on etched Si structures	Guo et al. [49]
Kapton	Dry etched nanowires	Zhu et al. [50]
PDMS	Convex dome shaped structures	Hou et al. [51]
Au	Nanoparticles	Zhu et al. [52]

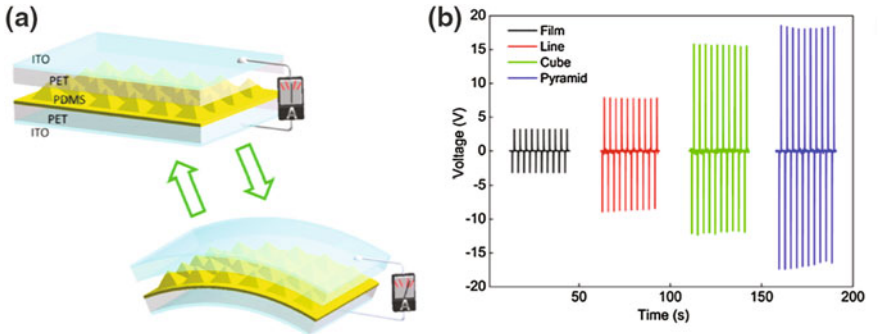

Fig. 2.16 **a** Schematic drawing of one of the early prototypes of triboelectric mechanism based energy harvester. **b** Voltage generated by the energy harvester using different topographies for patterned PDMS films [53]

self-powered pressure sensor which means the sensors do not need any external power source in order to operate as is required in the case of capacitive and piezoresistive sensors. In this Sect. 2.4, TENG devices have been reviewed based on different applications.

2.4.1 Biomechanical Energy Harvesters

Biomechanical energy is one of the most prevalent form of energy around human beings which can be used to power portable electronic devices like smartphones, watches and wearable sensors. Researchers have demonstrated various concepts and prototype devices to harvest biomechanical energy. Yang et al. [38] used an integrated rhombic gridded structure to harvest mechanical energy from vibrations generated from human walking (Fig. 2.17a). Rhombus shaped stacked structure used the hybridization of both contact-separation and sliding mode to enable contact electrification process. The TENG device was assembled on a backpack to develop a mobile source power for disaster relief workers, explorers in remote locations and field engineers. To harvest the energy directly from human heel strike, a low cost triboelectric energy harvester was developed by Bai et al. [47]. The device utilized multilayered zigzag structure in order to increase the effective contact area without significantly affecting the overall form factor of device (Fig. 2.17b). The device was assembled at the bottom of a common shoe and generated enough power to light up a few LEDs using the human walking motion. The energy harvesting device generated a maximum open circuit voltage of 215 V and a short circuit current of 0.66 mA. The maximum power density was reported to be 9.76 mW/cm^2.

Majority of the mechanical energy harvesting devices focus on harvesting energy from the external body movements like walking, hand movement etc. This energy can be used to power wearable sensors and small electronic devices. But as the technology advances, there will be many implanted sensors and devices being designed aimed at curing diseases, remote monitoring and aiding organs in functioning. Zheng et al. [54] proposed a breathing driven TENG to power in vivo devices such as pacemaker as shown in Fig. 2.18a. The device utilized micro pyramid patterned PDMS and aluminum metal layer as two triboelectric layers for energy generation. The device was also demonstrated for in vivo applications by implanting it on a living rat's diaphragm as shown in Fig. 2.18b. The implanted TENG generated a maximum power density of 8.44 mW m^{-2}, which was shown to drive a pacemaker device.

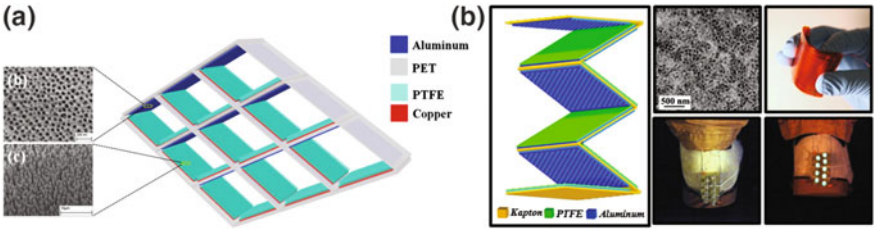

Fig. 2.17 **a** Rhombus shaped stacked structure to harvest mechanical energy from vibrations generated by human walking [38]. **b** Schematic diagram of the zigzag shaped multilayered triboelectric energy harvester; SEM micrograph of Al nanopores used one of the triboelectric layers; complete fabricated prototype of integrated multilayered triboelectric energy harvester [47]

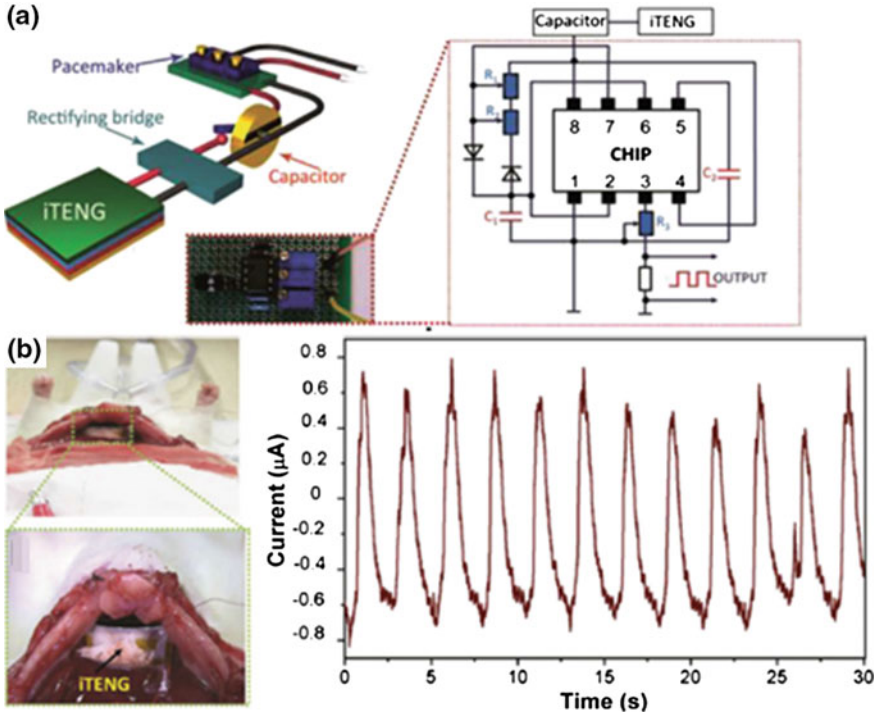

Fig. 2.18 Schematic diagram of the breathing driven TENG to power a pacemaker device [54]

2.4.2 Wind Based Energy Harvesters

Wind energy is a natural form of energy which has been used as a renewable source of energy to generate energy at a large scale. Conventional wind energy turbines used for large scale wind energy harvesting are bulky and require a huge capital investment to set up. Triboelectric mechanism can be used to generate electrical energy using wind energy at a smaller scale, which can be used to power wireless sensor nodes and electrical appliances. Xie et al. [55] demonstrated one of the first prototypes to harvest wind energy based on triboelectric mechanism as shown in Fig. 2.19a. The prototype device used a wind cup structure, which converted the wind flow energy into rotational kinetic energy. This rotational kinetic energy was then utilized to enable contact electrification between polytetrafluoroethylene (PTFE) nanowire-like structure and aluminum layer. The device generated a maximum power of 62.5 mW at a wind speed of 15 m/s. A rotary sliding mechanism based TENG was demonstrated by Zhu et al. [56] with a high power output of 1.5 W. The device comprised of a rotator and stator as shown in Fig. 2.19b. The stator constituted of a fluorinated ethylene propylene (FEP) layer with micro-patterned complementary sectors as electrode. The rotor was fabricated using

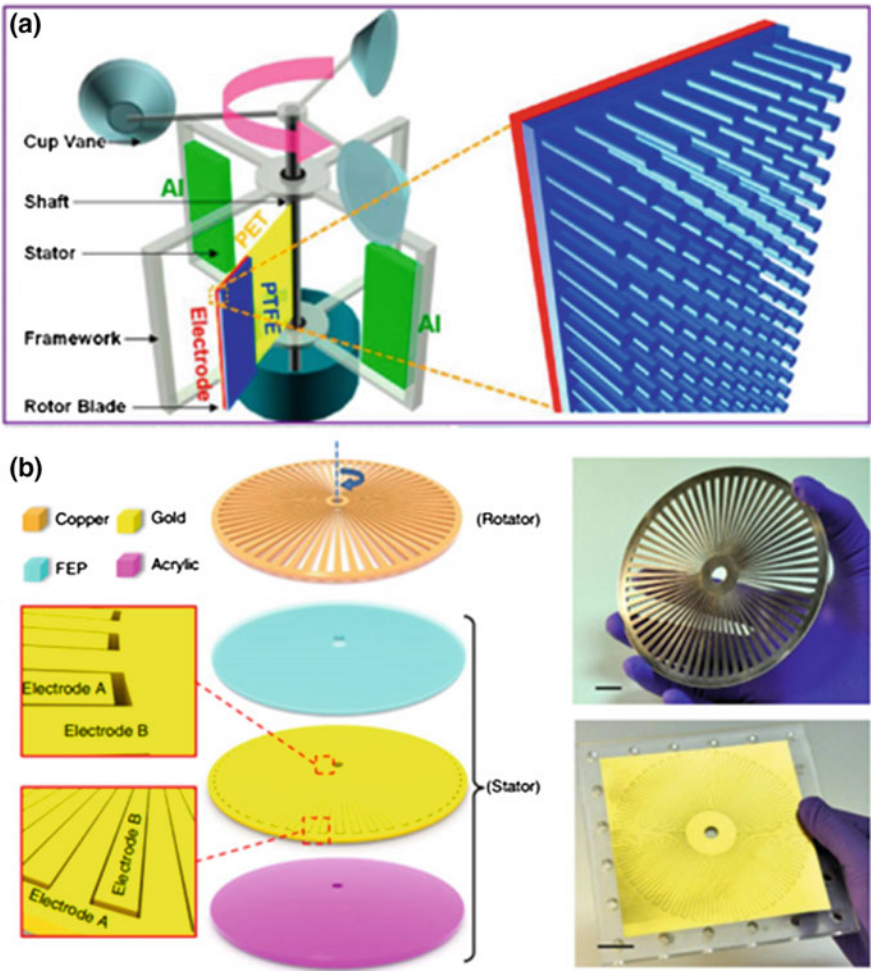

Fig. 2.19 **a** Wind-cup structure based TENG [55]. **b** High output TENG using micro-sector structures [56]

copper which acted as a triboelectric layer in conjunction with FEP. TENG was demonstrated to effectively harvest energy from air flow and water flow. Chen et al. [57] also demonstrated a rotary sliding mechanism based TENG which was shown to generate enough voltage for oxidation of sulphur dioxide, which has applications in self-powered air cleaning systems.

Another type of wind based TENG devices use flutter motion to convert wind energy into electrical energy. Bae et al. [58] proposed a TENG device which enabled contact electrification using fluttering motion of a flexible triboelectric layer. The flexible triboelectric layer was fabricated using a gold coated woven fabric as shown in Fig. 2.20a. The device demonstrated that the fluttering flag

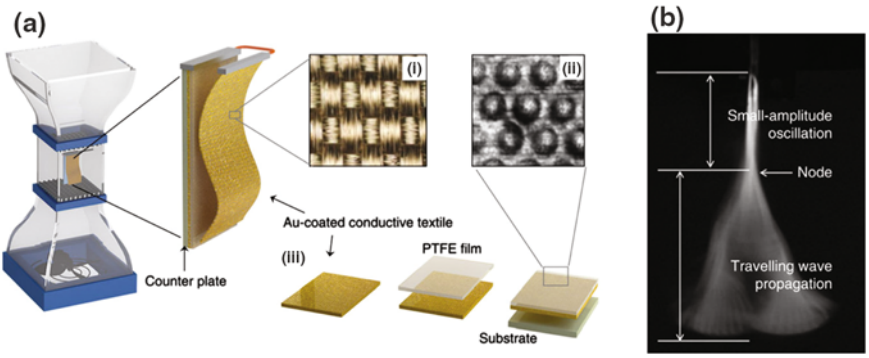

Fig. 2.20 **a** Schematic of the fluttering motion based wind energy harvester. **b** Fluttering motion of the flexible triboelectric layer captures using high speed camera [58]

motion can be utilized for small scale wind energy harvesting. It generated a maximum voltage of 250 V and current of 70 μA at a flow velocity of 22 ms^{-1}.

2.4.3 Water Based Energy Harvesters

Majority of TENG devices use solid materials such as dielectric polymers or metals as triboelectric layers to enable contact electrification phenomenon in order generate surface charge. In 2013, Lin et al. [59] demonstrated contact electrification between water and a PDMS layer. A device was fabricated in order to harvest mechanical energy which used water as one of the triboelectric layer. Patterned PDMS layer was chosen as another triboelectric layer due to its hydrophobic properties which aided in separation of water and PDMS during the contact electrification process. The working mechanism of the water based TENG is shown in Fig. 2.21a. During the contact electrification process due to contact separation motion between the two triboelectric layers enabled by external mechanical setup, water was observed to get positively charged as it donated electrons to PDMS layer. For the electrode corresponding to water as triboelectric layer, PMMA substrate coated with Cu was placed at the bottom of the experimental water tank. The experiments were conducted using deionized water, tap water and 0.6 M sodium chloride (NaCl) solution. The deionized water was shown to have a better performance as a triboelectric layer compared to tap water and NaCl solution. The performance for tap water and NaCl solution decreased due to the presence of electrolytes. As the water droplets cannot be completely prevented to form a layer on PDMS film, more positive charges including the dissolved ions in the water layer resulting into screening of negative surface charge generated on the PDMS film. Deionized water as a triboelectric layer along with patterned PDMS generated a charge density of 31.3 μQ m^{-2} during the contact electrification process. Lin et al. [60] fabricated a

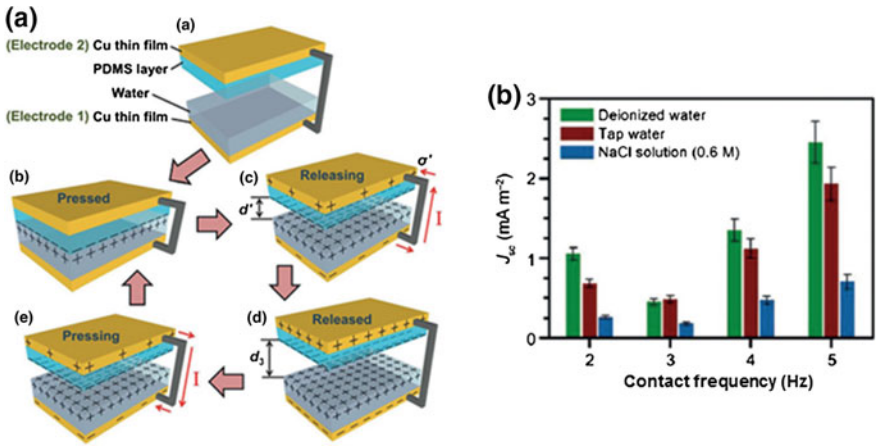

Fig. 2.21 **a** Operating mechanism of triboelectric energy harvester using water as triboelectric layer. **b** Current area density produced by different liquids as a triboelectric layer [59]

device to harvest energy using the charged water drops from rain or pipes. The device used PTFE hierarchal micro/nanostructures for contact electrification process with water drops. The device generated a peak voltage of 9.3 V and a peak current of 17 μA. Liang et al. [61] have demonstrated a prototype of transparent water based TENG which could be assembled on the windows in order to harvest energy from rainwater.

Apart from using water as a triboelectric layer, another method to harvest energy from water is utilizing the water's mechanical energy to enable contact electrification between two triboelectric layers. Yang et al. [62] demonstrated a TENG device, which used PTFE and polyamide (PA) as triboelectric layers. The device was fully enclosed in a spherical shell (Fig. 2.22) and was shown to harvest energy from water waves. Chen et al. [63] proposed the concept of network of small water wave energy harvester unit (Fig. 2.23a) to produce electricity at a large scale from sea/ocean waves. As per calculations, it was shown that power output of up to 1.15 MW can be generated from a water area of 1 km^2.

2.4.4 Wearable Energy Harvesters

Wearable energy harvesting devices which can harvest energy from human activities, are a solution to potentially power the wearable devices. One of the major direction of research in the area of wearable energy harvesters is focused towards textile or fabric based nanogenerators. Fabric based nanogenerators can camouflage with the clothes and also utilize large area of clothes for high power output. Kim et al. [64], demonstrated a stretchable weaved fabric for wearable energy harvesting applications. The fibers used to weave the fabric utilized PDMS tubes with high

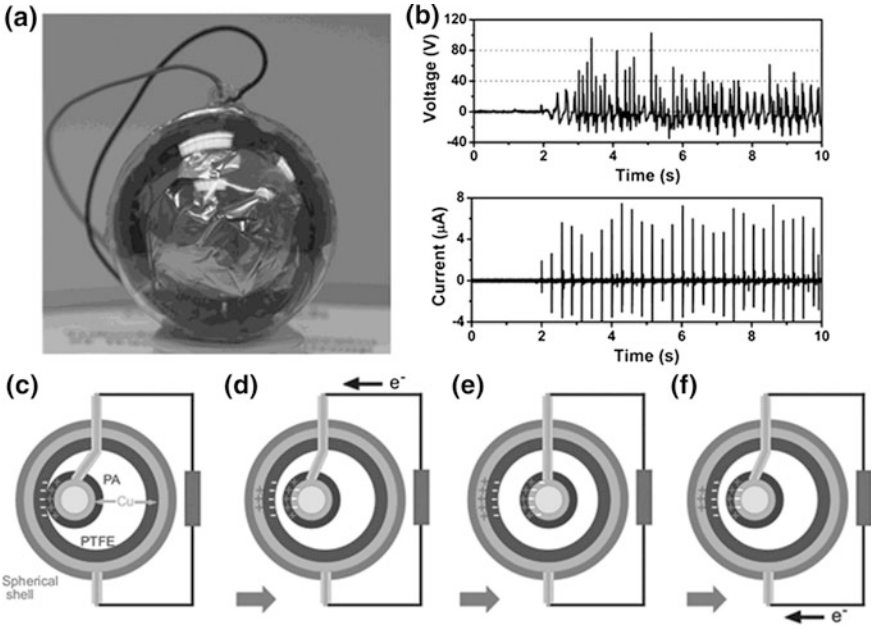

Fig. 2.22 **a** Prototype of fully enclosed TENG to harvest energy from water waves. **b** Voltage and current generated by the device when shaken by hand. **c–f** Operating mechanism of the TENG [62]

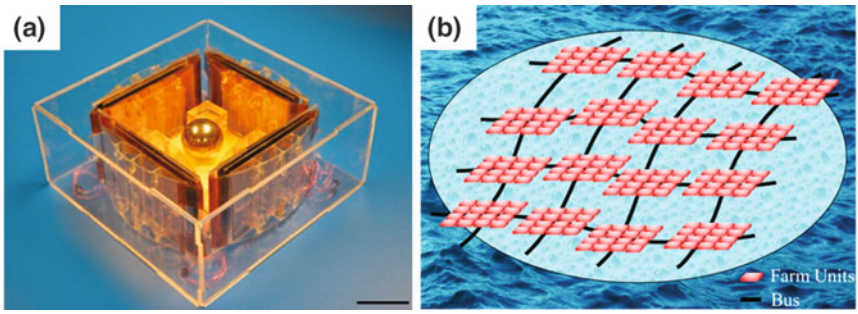

Fig. 2.23 **a** Single unit of water wave TENG. **b** A conceptual schematic of network or farm of unit TENGs to generate energy at a large scale [63]

aspect ratio nanostructured surface on the inner side and ZnO nanowires coated with Au as two triboelectric layers as shown in Fig. 2.24a. The weaved fabric with multiple fibers in an area of 14 cm × 14 cm generated a maximum voltage and current of 40 V and 210 μA, respectively. Seung et al. [65] demonstrated a fabric based TENG using a stacked structure of triboelectric layers as shown in Fig. 2.24b. A four layer stacked structure was shown to produce a peak voltage and current of 170 V and 120 μA, respectively.

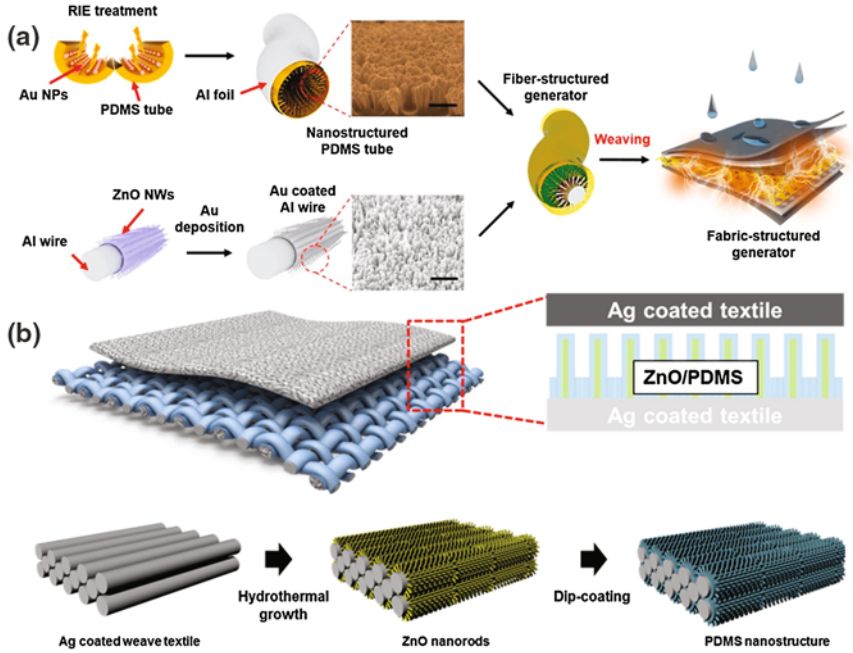

Fig. 2.24 **a** Fabric based TENG by weaving a fiber structured TENG [64]. **b** Fabric TENG by stacking of triboelectric layers [65]

Yang et al. [66] demonstrated a flexible TENG which utilized a wavy Kapton structure to enable contact electrification between a copper film and Kapton, as shown in Fig. 2.25. Due to the unique structure, the device could operate in both compressive and stretching mode. The device could generate a maximum voltage of up to 30 V from knee bending and straightening.

2.4.5 Self-powered Sensors

Sensors are an integral part of consumer and industrial electronic devices. Majority of these sensors work on the principle of measuring the change in properties such as capacitance and resistance. These sensors require external power supply in order to function. On the other hand, mechanical sensors to sense force, pressure or vibrations based on piezoelectric mechanisms do not require any external power for sensing as they have an ability to generate an electrical signal in response to a mechanical stimulation. Similarly, triboelectric mechanism can also generate an electrical signal when stimulated with an external mechanical force. These sensors

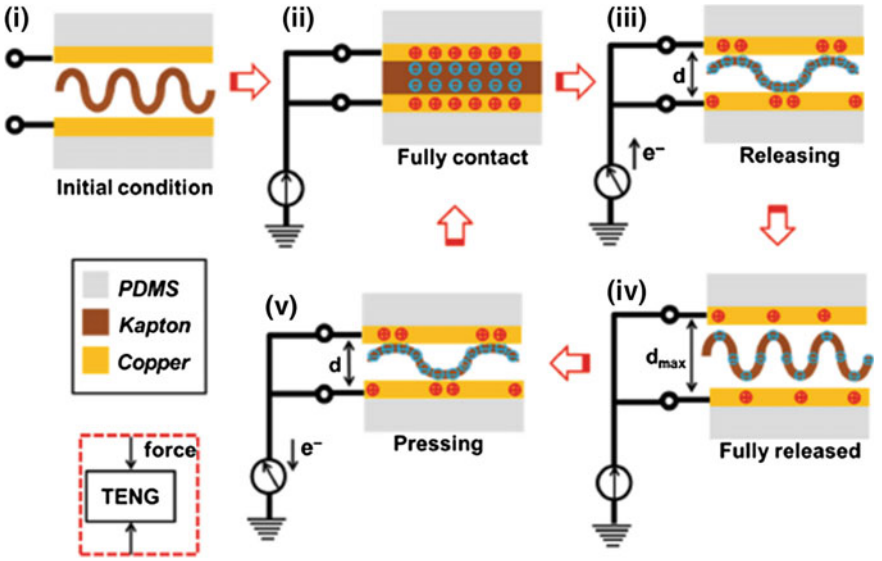

Fig. 2.25 Operating mechanism of the wavy structure based flexible TENG for wearable applications [66]

can be categorized as self-powered active sensors as they do not require an external power supply for sensing. Various kind of sensors have been realized by researchers using triboelectric mechanism and are reviewed in the following sections.

2.4.5.1 Tactile and Pressure Sensors

Yang et al. [67] demonstrated a self-powered tactile sensor array as shown in Fig. 2.26a. The device was designed for touch pad applications. It utilized micro-patterned PDMS as one of the triboelectric layers. As bare human finger touched the PDMS pixels, the electrons were injected from skin to PDMS due to contact electrification. Indium Tin Oxide (ITO) was used as an electrode beneath PDMS film to collect charged using triboelectric mechanism. The detection sensitivity of the pressure for every pixel was shown to be 0.29 ± 0.02 V kPa^{-1}. A similar device was also demonstrated by Meng et al. [68], which was shown to powered a liquid crystal display (LCD) screen.

Zhu et al. [69] fabricated a self-powered pressure sensor with a sensitivity of 44 V kPa^{-1} (Fig. 2.27a). The device was tested for durability and showed stable output for 10^5 cycles.

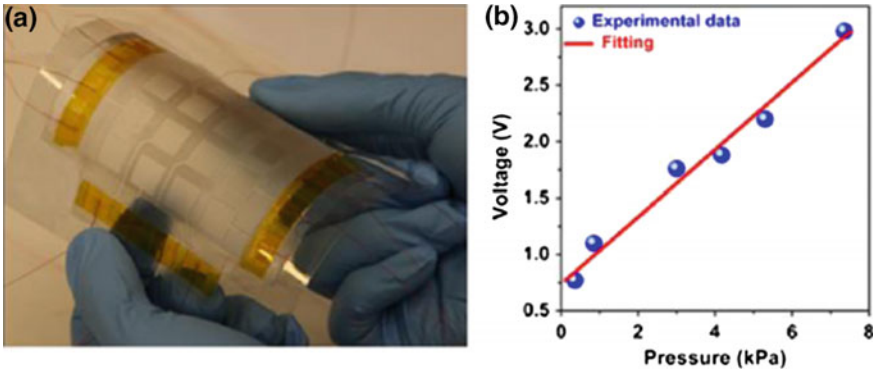

Fig. 2.26 **a** A photograph of the tactile sensor array. **b** Plot of the output voltage versus pressure [67]

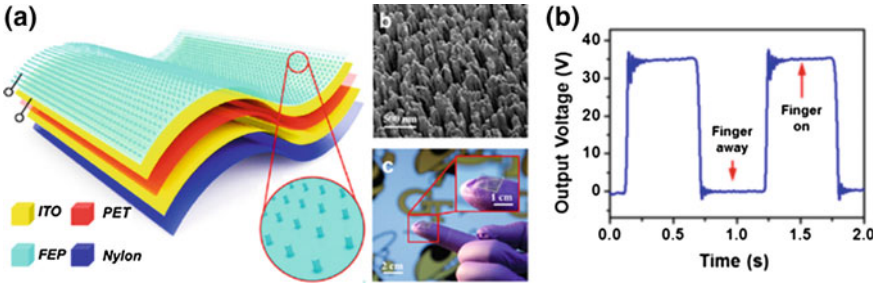

Fig. 2.27 **a** Schematic of the self-powered pressure sensor, SEM image of the polymer nanowires and a photograph of the fabricated sensor. **b** Output voltage produced by the sensor due to finger tapping [69]

2.4.5.2 Motion Tracking Sensors

Sensors based on triboelectric mechanism can also be utilized to sense motion parameters such as displacement, velocity and acceleration. Zhou et al. [70] proposed a grating based structure for motion sensing as shown in Fig. 2.28a. The structure comprised of parylene and silicon dioxide (SiO_2) gratings which underwent sliding motion relative to each other. Due to relative sliding motion of the two triboelectric layers, the two gratings experienced full overlap, partial separation and full separation. As the relative position of the two gratings changes, the open circuit potential between the ITO and Al electrode changes periodically. The data collected from the relative potential difference between electrodes and gap between the consecutive gratings was used to calculate the displacement with a resolution of 173 nm. Using the contact electrification effect and electrostatic induction between patterned electrodes, Wu et al. [71] designed a self-powered sensor for angular motion measurement (Fig. 2.28b).

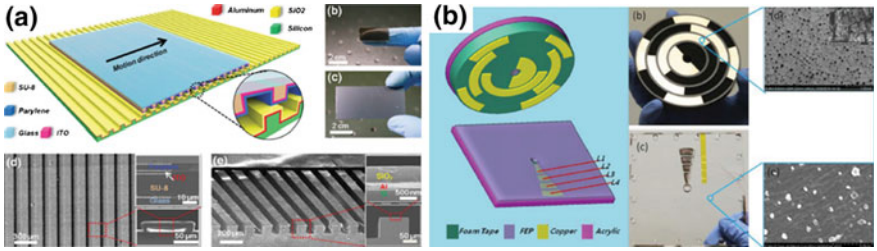

Fig. 2.28 **a** Triboelectric motion sensor using dual grating design [70]. **b** Schematic and photograph of the self-powered angular motion sensor [71]

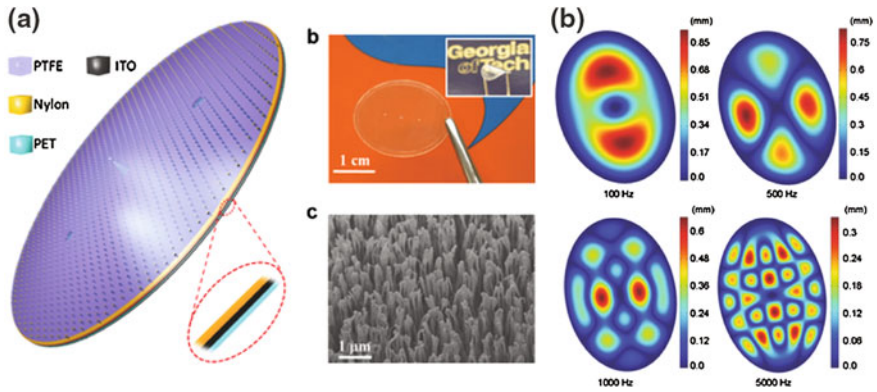

Fig. 2.29 **a** Eardrum inspired design of the voice recognition sensor. **b** Membrane vibrations simulated for different applied vibrations [72]

Various other self-powered mechanical sensors have been designed utilizing the triboelectric effect. Yang et al. [72] fabricated a self-powered voice recognition sensor using an eardrum inspired diaphragm design as shown in Fig. 2.29a. The sensor was also demonstrated for sensing arterial pulse wave for biometric recognition. Chen et al. [73] demonstrated a vibration sensor to sense vibration in the range of 0–200 Hz.

2.4.5.3 Chemical Sensors

Apart from mechanical sensing, triboelectric mechanism can also be used to detect chemical changes as the contact electrification phenomenon is affected by the chemical composition of the triboelectric layers. Several sensors have been demonstrated by the researchers using this principle. Lin et al. [74] detected the concentration of mercury ions (Hg^{2+}) with Tris-borate used as a buffer solution. The triboelectric layers comprised of a PDMS film and Au nanoparticles deposited onto an Au film. To enable the selective detection of Hg^{2+}, 3-mercaptopropionic acid

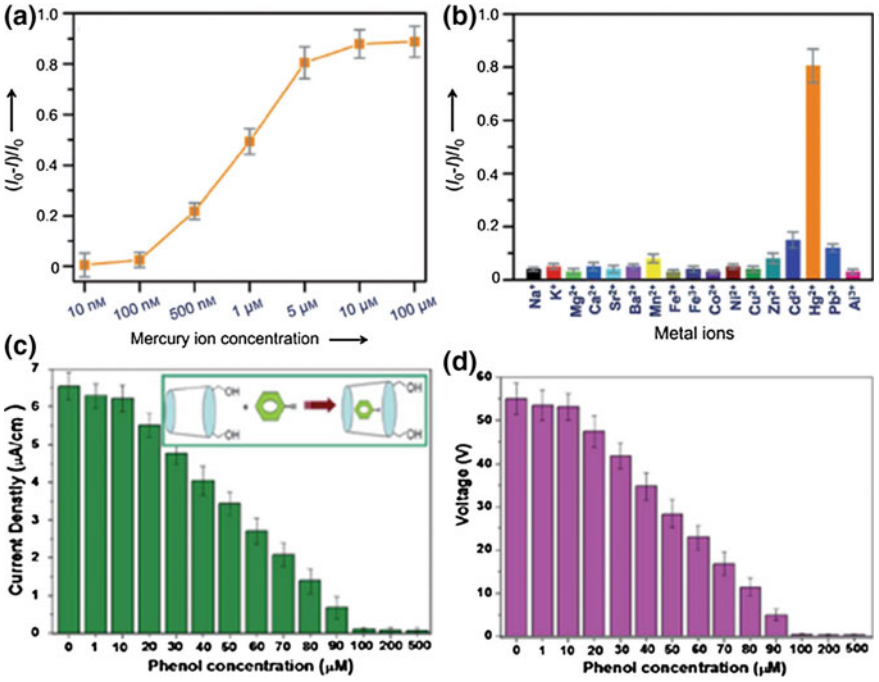

Fig. 2.30 **a** Sensitivity of the self-powered Hg^{2+} ion sensor. **b** Plot depicting the selectivity of the device for Hg^{2+}. The concentration of all metal ions tested was 5 μM [74]. **c** Current and **d** voltage signals from the sensor for various phenol concentrations [75]

(3-MPA) was self-assembled onto the surface of Au nanoparticles using strong Au-S interaction. The change in the performance of TENG resulted due to difference in triboelectric polarities of Au nanoparticles and Hg^{2+} ions. The device had a detection limit of 30 nM and linear range between 100 nM and 5 μM (Fig. 2.30a). The device was also shown to have high selectivity for Hg^{2+} ions. Li et al. [75] demonstrated a self-powered phenol detection sensor using titanium dioxide (TiO_2) nanowires and PTFE as triboelectric layers. β-cyclodextrin molecules were assembled onto TiO_2 nanowire layer, which acted as the phenol recognition element and also improved the performance of the contact electrification. The device achieved a detection sensitivity of 0.01 μM^{-1} by calibrating the current and voltage signals in the range of 10–100 μM.

2.5 Summary

In this chapter, various mechanical energy harvesting technologies have been reviewed. The applications of triboelectric devices in harvesting mechanical energy available in different forms has been reviewed. Thereafter, various self-powered

devices based on triboelectric effect have been discussed including tactile sensing, motion sensing and chemical sensing.

References

1. T. Ikeda, *Fundamentals of Piezoelectricity* (Oxford University Press, Oxford, 1996)
2. S. Roundy, P.K. Wright, A piezoelectric vibration based generator for wireless electronics. Smart Mater. Struct. **13**, 1131 (2004)
3. N. White, P. Glynne-Jones, S. Beeby, A novel thick-film piezoelectric micro-generator. Smart Mater. Struct. **10**, 850–852 (2001)
4. M. Renaud, K. Karakaya, T. Sterken, P. Fiorini, C. Van Hoof, R. Puers, Fabrication, modelling and characterization of MEMS piezoelectric vibration harvesters. Sens. Actuators, A **145**, 380–386 (2008)
5. J.-Q. Liu, H.-B. Fang, Z.-Y. Xu, X.-H. Mao, X.-C. Shen, D. Chen et al., A MEMS-based piezoelectric power generator array for vibration energy harvesting. Microelectron. J. **39**, 802–806 (2008)
6. J. Kymissis, C. Kendall, J. Paradiso, N. Gershenfeld, Parasitic Power Harvesting in Shoes, in *Digest of Papers. Second International Symposium on Wearable Computers 1998*, 1998, pp. 132–139
7. S. Priya, Modeling of electric energy harvesting using piezoelectric windmill. Appl. Phys. Lett. **87**, 184101 (2005)
8. Z.L. Wang, J. Song, Piezoelectric nanogenerators based on zinc oxide nanowire arrays. Science **312**, 242–246 (2006)
9. X. Wang, J. Song, J. Liu, Z.L. Wang, Direct-current nanogenerator driven by ultrasonic waves. Science **316**, 102–105 (2007)
10. S.Y. Chung, S. Kim, J.H. Lee, K. Kim, S.W. Kim, C.Y. Kang et al., All-solution-processed flexible thin film piezoelectric nanogenerator. Adv. Mater. **24**, 6022–6027 (2012)
11. S. Lee, S.H. Bae, L. Lin, Y. Yang, C. Park, S.W. Kim et al., Super-flexible nanogenerator for energy harvesting from gentle wind and as an active deformation sensor. Adv. Funct. Mater. **23**, 2445–2449 (2013)
12. L. Lin, Y. Hu, C. Xu, Y. Zhang, R. Zhang, X. Wen et al., Transparent flexible nanogenerator as self-powered sensor for transportation monitoring. Nano Energy **2**, 75–81 (2013)
13. C. Williams, C. Shearwood, M. Harradine, P. Mellor, T. Birch, R. Yates, Development of an Electromagnetic Micro-Generator, in *IEE Proceedings on Circuits, Devices and Systems,* 2001, pp. 337–342
14. J.M. Lee, S.C. Yuen, W.J. Li, P.H. Leong, Development of an AA Size Energy Transducer with Micro Resonators, in *ISCAS'03 Proceedings of the 2003 International Symposium on Circuits and Systems, 2003*, vol. 4, 2003, pp. IV-876–IV-879
15. N.N. Ching, H. Wong, W.J. Li, P.H. Leong, Z. Wen, A laser-micromachined multi-modal resonating power transducer for wireless sensing systems. Sens. Actuators, A **97**, 685–690 (2002)
16. C. Cepnik, U. Wallrabe, A flat high performance micro energy harvester based on a serpentine coil with a single winding, in *Solid-State Sensors, Actuators and Microsystems Conference (TRANSDUCERS), 2011 16th International*, 2011, pp. 661–664
17. B. Yang, C. Lee, W. Xiang, J. Xie, J.H. He, R.K. Kotlanka et al., Electromagnetic energy harvesting from vibrations of multiple frequencies. J. Micromech. Microeng. **19**, 035001 (2009)
18. S. Kulkarni, E. Koukharenko, R. Torah, J. Tudor, S. Beeby, T. O'Donnell et al., Design, fabrication and test of integrated micro-scale vibration-based electromagnetic generator. Sens. Actuators, A **145**, 336–342 (2008)

19. J.M. Donelan, Q. Li, V. Naing, J. Hoffer, D. Weber, A.D. Kuo, Biomechanical energy harvesting: generating electricity during walking with minimal user effort. Science **319**, 807–810 (2008)
20. E. Halvorsen, S.D. Nguyen, MEMS Electrostatic Energy Harvesters with Nonlinear Springs, in *Advances in Energy Harvesting Methods*, (Springer, Berlin, 2013), pp. 63–90
21. S. Meninger, J.O. Mur-Miranda, R. Amirtharajah, A.P. Chandrakasan, J.H. Lang, Vibration-to-electric energy conversion. IEEE Trans. Very Large Scale Integ. (VLSI) Syst. **9**, 64–76 (2001)
22. D. Hoffmann, B. Folkmer, Y. Manoli, Analysis and characterization of triangular electrode structures for electrostatic energy harvesting. J. Micromech. Microeng. **21**, 104002 (2011)
23. B. Yang, C. Lee, R.K. Kotlanka, J. Xie, S.P. Lim, A MEMS rotary comb mechanism for harvesting the kinetic energy of planar vibrations. J. Micromech. Microeng. **20**, 065017 (2010)
24. D. Nguyen, E. Halvorsen, G. Jensen, A. Vogl, Fabrication and characterization of a wideband MEMS energy harvester utilizing nonlinear springs. J. Micromech. Microeng. **20**, 125009 (2010)
25. S.D. Nguyen, E. Halvorsen, Nonlinear springs for bandwidth-tolerant vibration energy harvesting. J. Microelectromech. Syst. **20**, 1225–1227 (2011)
26. J. Boland, Y.-H. Chao, Y. Suzuki, Y. Tai, Micro Electret Power Generator, in *IEEE the Sixteenth Annual International Conference on Micro Electro Mechanical Systems, 2003. MEMS-03 Kyoto*, 2003, pp. 538–541
27. T. Tsutsumino, Y. Suzuki, N. Kasagi, Y. Sakane, Seismic power generator using high-performance polymer electret, in *19th IEEE International Conference on Micro Electro Mechanical Systems, 2006. MEMS 2006 Istanbul*, 2006, pp. 98–101
28. Y. Sakane, Y. Suzuki, N. Kasagi, The development of a high-performance perfluorinated polymer electret and its application to micro power generation. J. Micromech. Microeng. **18**, 104011 (2008)
29. S. Matsusaka, H. Maruyama, T. Matsuyama, M. Ghadiri, Triboelectric charging of powders: a review. Chem. Eng. Sci. **65**, 5781–5807 (2010)
30. W. Harper, The Volta effect as a cause of static electrification, in *Proceedings of the Royal Society of London. Series A. Mathematical and Physical Sciences,* vol. 205, 1951, pp. 83–103
31. D. Davies, Charge generation on dielectric surfaces. J. Phys. D Appl. Phys. **2**, 1533 (1969)
32. Y. Murata, S. Kittaka, Evidence of electron transfer as the mechanism of static charge generation by contact of polymers with metals. Jpn. J. Appl. Phys. **18**, 421 (1979)
33. J. Henniker, Triboelectricity in polymers. Nature **196**, 474 (1962)
34. A. Diaz, R. Felix-Navarro, A semi-quantitative tribo-electric series for polymeric materials: the influence of chemical structure and properties. J. Electrostat. **62**, 277–290 (2004)
35. S. Niu, S. Wang, L. Lin, Y. Liu, Y.S. Zhou, Y. Hu et al., Theoretical study of contact-mode triboelectric nanogenerators as an effective power source. Energy Environ. Sci. **6**, 3576–3583 (2013)
36. S. Niu, Y. Liu, S. Wang, L. Lin, Y.S. Zhou, Y. Hu et al., Theory of sliding-mode triboelectric nanogenerators. Adv. Mater. **25**, 6184–6193 (2013)
37. Z.-H. Lin, Y. Xie, Y. Yang, S. Wang, G. Zhu, Z.L. Wang, Enhanced triboelectric nanogenerators and triboelectric nanosensor using chemically modified TiO_2 nanomaterials. ACS Nano **7**, 4554–4560 (2013)
38. W. Yang, J. Chen, G. Zhu, J. Yang, P. Bai, Y. Su et al., Harvesting energy from the natural vibration of human walking. ACS Nano **7**, 11317–11324 (2013)
39. G. Cheng, Z.-H. Lin, L. Lin, Z.-L. Du, Z.L. Wang, Pulsed nanogenerator with huge instantaneous output power density. ACS Nano **7**, 7383–7391 (2013)
40. M. Han, X.-S. Zhang, B. Meng, W. Liu, W. Tang, X. Sun et al., r-Shaped hybrid nanogenerator with enhanced piezoelectricity. ACS Nano **7**, 8554–8560 (2013)
41. Y. Yang, H. Zhang, Y. Liu, Z.-H. Lin, S. Lee, Z. Lin et al., Silicon-based hybrid energy cell for self-powered electrodegradation and personal electronics. ACS Nano **7**, 2808–2813 (2013)

42. Y. Yang, H. Zhang, J. Chen, Q. Jing, Y.S. Zhou, X. Wen et al., Single-electrode-based sliding triboelectric nanogenerator for self-powered displacement vector sensor system. ACS Nano **7**, 7342–7351 (2013)
43. L. Lin, Y. Xie, S. Wang, W. Wu, S. Niu, X. Wen et al., Triboelectric active sensor array for self-powered static and dynamic pressure detection and tactile imaging. ACS Nano **7**, 8266–8274 (2013)
44. Y. Yang, G. Zhu, H. Zhang, J. Chen, X. Zhong, Z.-H. Lin et al., Triboelectric nanogenerator for harvesting wind energy and as self-powered wind vector sensor system. ACS Nano **7**, 9461–9468 (2013)
45. Q. Jing, G. Zhu, P. Bai, Y. Xie, J. Chen, R.P. Han et al., Case-encapsulated triboelectric nanogenerator for harvesting energy from reciprocating sliding motion. ACS Nano **8**, 3836–3842 (2014)
46. Y. Yang, L. Lin, Y. Zhang, Q. Jing, T.-C. Hou, Z.L. Wang, Self-powered magnetic sensor based on a triboelectric nanogenerator. ACS Nano **6**, 10378–10383 (2012)
47. P. Bai, G. Zhu, Z.-H. Lin, Q. Jing, J. Chen, G. Zhang et al., Integrated multilayered triboelectric nanogenerator for harvesting biomechanical energy from human motions. ACS Nano **7**, 3713–3719 (2013)
48. W. Du, X. Han, L. Lin, M. Chen, X. Li, C. Pan et al., A three dimensional multi-layered sliding triboelectric nanogenerator, Adv. Energy Mater. 4(11), (2014)
49. H. Guo, X. He, J. Zhong, Q. Zhong, Q. Leng, C. Hu et al., A nanogenerator for harvesting airflow energy and light energy. J. Mater. Chem. A **2**, 2079–2087 (2014)
50. G. Zhu, C. Pan, W. Guo, C.-Y. Chen, Y. Zhou, R. Yu et al., Triboelectric-generator-driven pulse electrodeposition for micropatterning. Nano Lett. **12**, 4960–4965 (2012)
51. T.-C. Hou, Y. Yang, H. Zhang, J. Chen, L.-J. Chen, Z. Lin Wang, Triboelectric nanogenerator built inside shoe insole for harvesting walking energy. Nano Energy **2**, 856–862 (2013)
52. G. Zhu, Z.-H. Lin, Q. Jing, P. Bai, C. Pan, Y. Yang et al., Toward large-scale energy harvesting by a nanoparticle-enhanced triboelectric nanogenerator. Nano Lett. **13**, 847–853 (2013)
53. F.-R. Fan, L. Lin, G. Zhu, W. Wu, R. Zhang, Z.L. Wang, Transparent triboelectric nanogenerators and self-powered pressure sensors based on micropatterned plastic films. Nano Lett. **12**, 3109–3114 (2012)
54. Q. Zheng, B. Shi, F. Fan, X. Wang, L. Yan, W. Yuan et al., In vivo powering of pacemaker by breathing-driven implanted triboelectric nanogenerator. Adv. Mater. **26**, 5851–5856 (2014)
55. Y. Xie, S. Wang, L. Lin, Q. Jing, Z.-H. Lin, S. Niu et al., Rotary triboelectric nanogenerator based on a hybridized mechanism for harvesting wind energy. ACS Nano **7**, 7119–7125 (2013)
56. G. Zhu, J. Chen, T. Zhang, Q. Jing, Z.L. Wang, Radial-arrayed rotary electrification for high performance triboelectric generator. Nat. Commun. **5** (2014)
57. S. Chen, C. Gao, W. Tang, H. Zhu, Y. Han, Q. Jiang et al., Self-powered cleaning of air pollution by wind driven triboelectric nanogenerator, Nano Energy **14**, 217–225 (2014)
58. J. Bae, J. Lee, S. Kim, J. Ha, B.-S. Lee, Y. Park et al., Flutter-driven triboelectrification for harvesting wind energy. Nat. Commun. **5** (2014)
59. Z.H. Lin, G. Cheng, L. Lin, S. Lee, Z.L. Wang, Water–solid surface contact electrification and its use for harvesting liquid-wave energy. Angew. Chem. Int. Ed. **52**, 12545–12549 (2013)
60. Z.H. Lin, G. Cheng, S. Lee, K.C. Pradel, Z.L. Wang, Harvesting water drop energy by a sequential contact-electrification and electrostatic-induction process. Adv. Mater. **26**, 4690–4696 (2014)
61. Q. Liang, X. Yan, Y. Gu, K. Zhang, M. Liang, S. Lu et al., Highly transparent triboelectric nanogenerator for harvesting water-related energy reinforced by antireflection coating. Sci. Rep. **5** (2015)
62. Y. Yang, H. Zhang, R. Liu, X. Wen, T.C. Hou, Z.L. Wang, Fully enclosed triboelectric nanogenerators for applications in water and harsh environments. Adv. Energy Mater. **3**, 1563–1568 (2013)

63. J. Chen, J. Yang, Z. Li, X. Fan, Y. Zi, Q. Jing et al., Networks of triboelectric nanogenerators for harvesting water wave energy: a potential approach toward blue energy. ACS Nano **9**, 3324–3331 (2015)
64. K.N. Kim, J. Chun, J.W. Kim, K.Y. Lee, J.-U. Park, S.-W. Kim et al., Highly stretchable two-dimensional fabrics for wearable triboelectric nanogenerator under harsh environments. ACS Nano 2015
65. W. Seung, M.K. Gupta, K.Y. Lee, K.-S. Shin, J.-H. Lee, T.Y. Kim et al., Nanopatterned textile-based wearable triboelectric nanogenerator. ACS Nano **9**, 3501–3509 (2015)
66. P.K. Yang, L. Lin, F. Yi, X. Li, K.C. Pradel, Y. Zi et al., A flexible, stretchable and shape adaptive approach for versatile energy conversion and self powered biomedical monitoring. Adv. Mater. **27**, 3817–3824 (2015)
67. Y. Yang, H. Zhang, Z.-H. Lin, Y.S. Zhou, Q. Jing, Y. Su et al., Human skin based triboelectric nanogenerators for harvesting biomechanical energy and as self-powered active tactile sensor system. ACS Nano **7**, 9213–9222 (2013)
68. B. Meng, W. Tang, Z.-H. Too, X. Zhang, M. Han, W. Liu et al., A transparent single-friction-surface triboelectric generator and self-powered touch sensor. Energy Environ. Sci. **6**, 3235–3240 (2013)
69. G. Zhu, W.Q. Yang, T. Zhang, Q. Jing, J. Chen, Y.S. Zhou et al., Self-powered, ultrasensitive, flexible tactile sensors based on contact electrification. Nano Lett. **14**, 3208–3213 (2014)
70. Y.S. Zhou, G. Zhu, S. Niu, Y. Liu, P. Bai, Q. Jing et al., Nanometer resolution self-powered static and dynamic motion sensor based on micro-grated triboelectrification. Adv. Mater. **26**, 1719–1724 (2014)
71. Y. Wu, Q. Jing, J. Chen, P. Bai, J. Bai, G. Zhu et al., A self-powered angle measurement sensor based on triboelectric nanogenerator. Adv. Funct. Mater. **25**, 2166–2174 (2015)
72. J. Yang, J. Chen, Y. Su, Q. Jing, Z. Li, F. Yi et al., Eardrum-inspired active sensors for self-powered cardiovascular system characterization and throat-attached anti-interference voice recognition. Adv. Mater. **27**, 1316–1326 (2015)
73. J. Chen, G. Zhu, W. Yang, Q. Jing, P. Bai, Y. Yang et al., Harmonic-resonator-based triboelectric nanogenerator as a sustainable power source and a self-powered active vibration sensor. Adv. Mater. **25**, 6094–6099 (2013)
74. Z.H. Lin, G. Zhu, Y.S. Zhou, Y. Yang, P. Bai, J. Chen et al., A self-powered triboelectric nanosensor for mercury ion detection. Angew. Chem. Int. Ed. **52**, 5065–5069 (2013)
75. Z. Li, J. Chen, J. Yang, Y. Su, X. Fan, Y. Wu et al., β-cyclodextrin enhanced triboelectrification for self-powered phenol detection and electrochemical degradation. Energy Environ. Sci. **8**, 887–896 (2015)